Supporting Information

Rapidly tuning electrocatalytic activity of perovskite oxides by plasma treatment

Zhu Sun,*[,1,3,5] Weiwei Fan,*[,2,4,5] Tianquan Lin[1,3]

[1]School of Materials Science and Engineering, Shanghai Jiao Tong University, 800 Dongchuan Road, Shanghai, 200240, China

[2]Key Laboratory of Energy Thermal Conversion and Control of Ministry of Education, School of Energy and Environment, Southeast University, Nanjing 210096, China

[3]Zhangjiang Institute for Advanced Study (ZIAS), Shanghai Jiao Tong University, Shanghai, 201210, China

[4]Department of Nuclear Science and Engineering, Massachusetts Institute of Technology, Cambridge 02139, USA

[5]These authors contributed equally to this work.

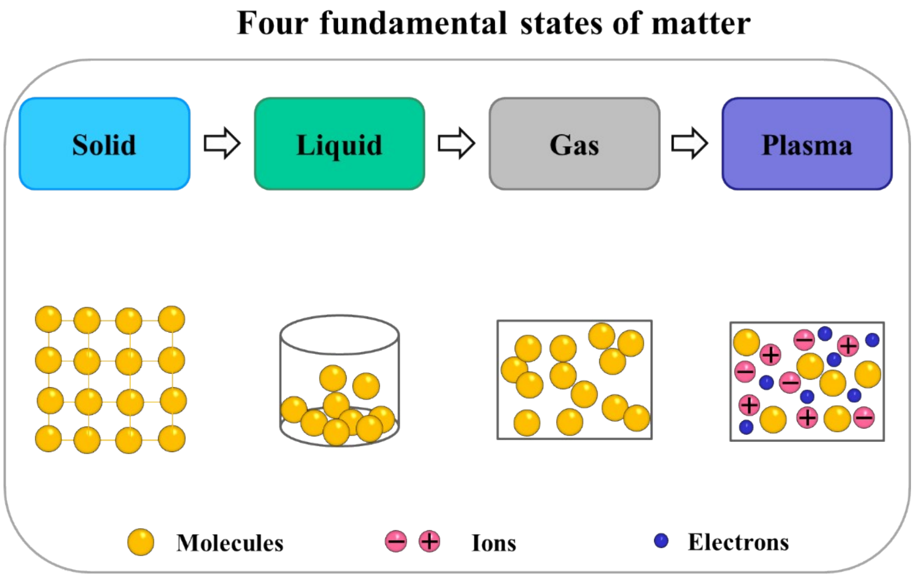

Figure S1. Illustration of the four fundamental states of matter.

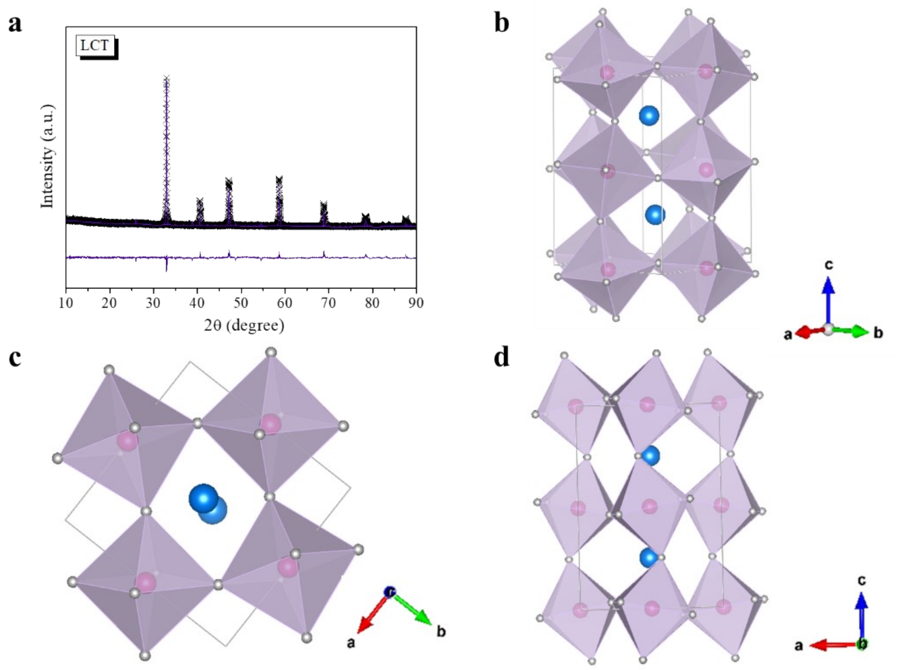

Figure S2. **a,** Rietveld refinement XRD profile of the as-synthesized LCT oxide. **b,c,d,** Crystal structural of LCT oxide at different views, where blue spheres denote La/Ca, pink spheres denote Ti, grey spheres denote O.

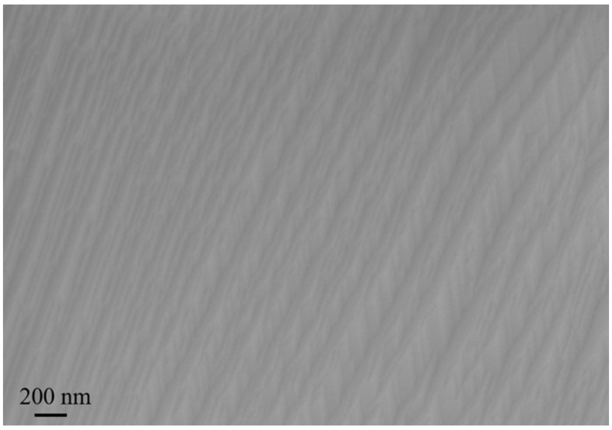

Figure S3. SEM image of the LCTN after thermal treatment at 350 °C for 1h in H_2.

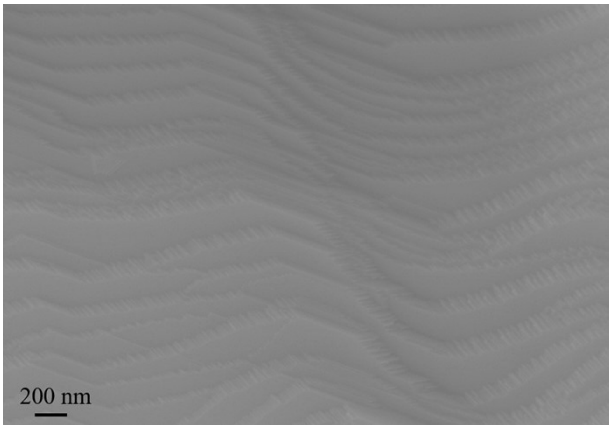

Figure S4. SEM image of the plasma-treated LCT.

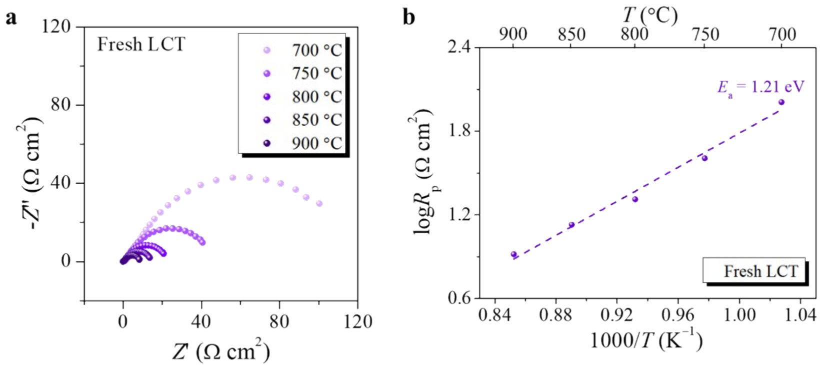

Figure S5. **a,** Nyquist plots of the fresh LCT electrode collected from 700 to 900 ℃ in hydrogen atmosphere under OCV conditions. **b,** Arrhenius plots of R_p for fresh LCT electrode.

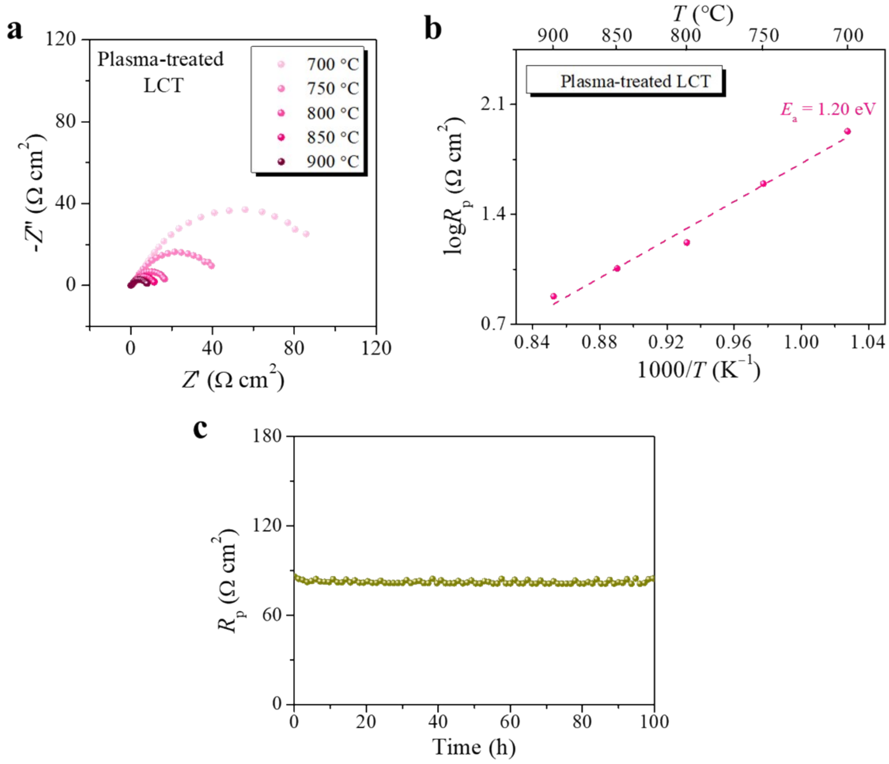

Figure S6. **a,** Nyquist plots of the plasma-treated LCT collected from 700 to 900 °C in hydrogen atmosphere under OCV conditions. **b,** Arrhenius plots of R_p of the plasma-treated LCT electrode. **c,** Time dependence of R_p collected at 700 °C in hydrogen atmosphere for the plasma-treated LCT.

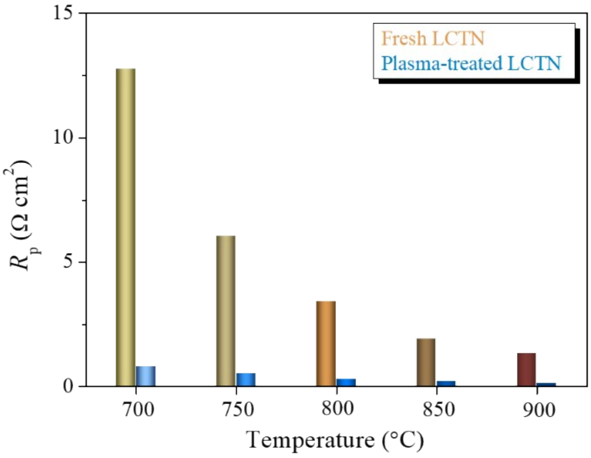

Figure S7. Comparison of R_p between the fresh LCTN and the plasma-treated LCTN at different temperatures.

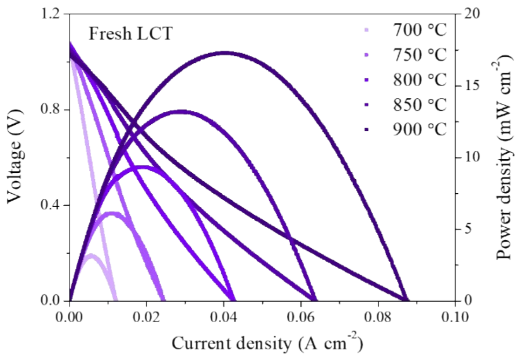

Figure S8. Voltage and power density versus current density for the cell LCT(fresh)|SSZ|LSM-SSZ measured from 700 to 900 °C using humidified H_2 as fuel and air as oxidant.

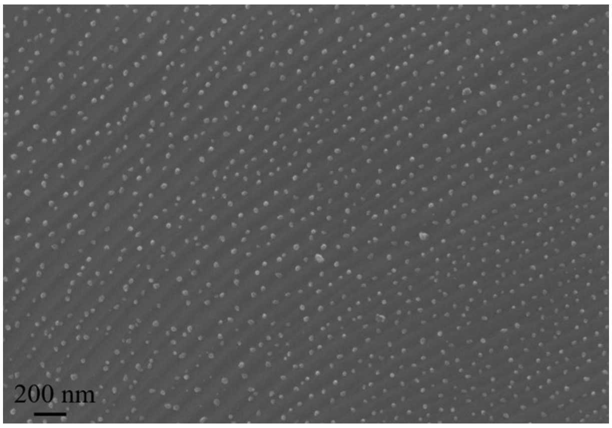

Figure S9. SEM image of the plasma-treated LCTN after stability test.

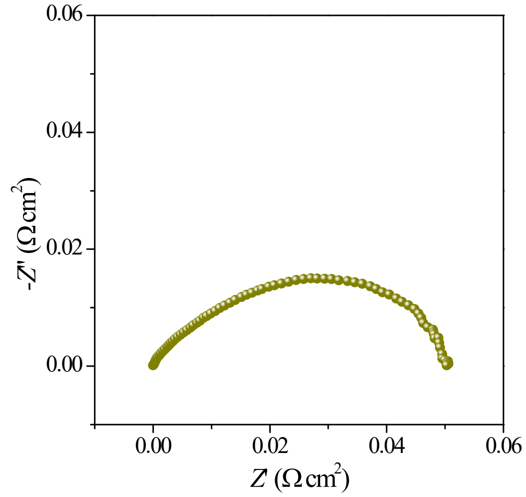

Figure S10. Nyquist plots of the half-cell LSM-SSZ|SSZ|LSM-SSZ collected at 900 ℃ under OCV condition in air.

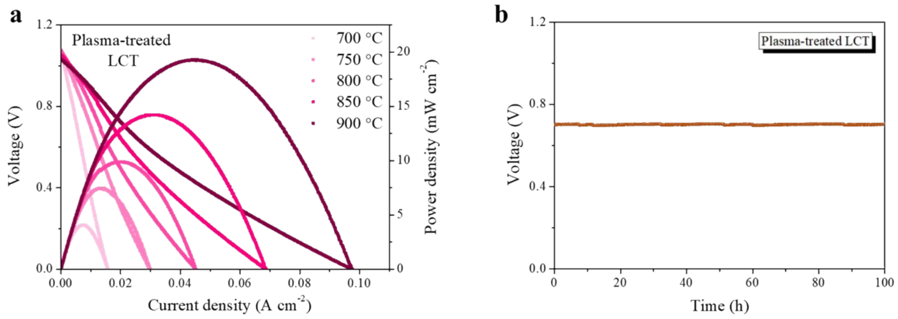

Figure S11. **a,** Voltage and power density versus current density for the cell LCT(plasma-treated)|SSZ|LSM-SSZ measured from 700 to 900 ℃ using humidified H_2 as fuel and air as oxidant. **b,** Cell voltage as a function of testing time for the single cell LCT(plasma-treated)|SSZ|LSM-SSZ at 700 °C.

Activation energy calculation:

Activation energy (E_a), associating with the electrochemical reaction mechanism including the processes of gas adsorption, dissociation and diffusion, can be calculated by the following equation.

$$\log R_p = \log R_0 - \frac{E_a}{2.303RT} \quad (1)$$

where R_0 is the pre-exponential factor, R is the gas constant (8.314 J mol^{-1} K^{-1}), T is the absolute temperature (K).

Table S1. Refined structural parameters for LCTN obtained by fitting of powder XRD data at room temperature.

Atoms, sites	Parameters	LCTN
	Space group	Pbnm (62)
	a (Å)	5.4642(4)
	b (Å)	7.7339(4)
	c (Å)	5.4633(7)
	V (Å^3)	230.87
La, 4c	*x*	0.4670
	y	0.2500
	z	0.0072
	Occupancy	0.43
Ca, 4c	*x*	0.4670
	y	0.2500
	z	0.0072
	Occupancy	0.37
Ti, 4a	*x*	0
	y	0
	z	0
	Occupancy	0.94
Ni, 4a	*x*	0
	y	0
	z	0
	Occupancy	0.06
O1, 4c	*x*	0.5107
	y	0.2500
	z	0.5722
	Occupancy	1
O1, 8d	*x*	0.2158
	y	0.0346
	z	0.2826
	Occupancy	1
	R_{wp}	16.68
	R_p	12.54
	χ^2	4.09

Table S2. Refined structural parameters for LCT obtained by fitting of powder XRD data at room temperature.

Atoms, sites	Parameters	LCT
	Space group	Pbnm (62)
	a (Å)	5.4587(5)
	b (Å)	7.7261(5)
	c (Å)	5.4562(4)
	V (Å^3)	230.11
La, 4c	*x*	0.4670
	y	0.2500
	z	0.0072
	Occupancy	0.43
Ca, 4c	*x*	0.4670
	y	0.2500
	z	0.0072
	Occupancy	0.37
Ti, 4a	*x*	0
	y	0
	z	0
	Occupancy	1
O1, 4c	*x*	0.5107
	y	0.2500
	z	0.5722
	Occupancy	1
O1, 8d	*x*	0.2158
	y	0.0346
	z	0.2826
	Occupancy	1
	R_{wp}	14.83
	R_p	10.19
	χ^2	3.01

$$M_xO_y + yH_2(g) \xrightarrow{\text{Reduction}} xM^0 + yH_2O(g) \quad (2)$$

Table S3 Thermodynamic parameters of reducing the corresponding oxide to metal at 900 °C

Metal oxides	ΔH (kJ)	ΔS (J K^{-1})	ΔG (kJ)	Equilibrium constant K
La_2O_3	1041.806	110.115	912.625	2.301E-41
CaO	395.428	56.933	328.637	2.324E-15
TiO_2	445.167	67.578	365.888	5.098E-17
NiO	−14.070	30.238	-49.544	1.607E+02

Table S4 Comparison of peak power density among different nanoparticle-decorated materials

Host oxide	Exsolved particle	Size (nm)	Exsolving time (h)	PPD ($W\ cm^{-2}$)
LCTN (this work)	Ni	16	0.25	1.1
$(Pr_{0.4}Sr_{0.6})_3(Fe_{0.85}Mo_{0.15})_2O_7$[1]	Co-Fe	80	2	0.5
$(LaSr)_{0.9}Fe_{0.9}Cu_{0.1}O_4$[2]	Cu	50	10	0.57
$La_{1.2}Sr_{0.8}Mn_{0.4}Fe_{0.6}O_{4-\delta}$[3]	Fe_3Co_2	30	20	0.63
$La_{0.95}Fe_{0.80}Ni_{0.05}Ti_{0.15}O_3$[4]	Ni	25	5	0.6
$Cu_{1-x}Ni_xFe_2O_4$[5]	Cu-Fe-Ni	60	1	0.67
$La_{0.8}Sr_{1.2}Fe_{0.9}Co_{0.1}O_{4\pm\delta}$[6]	Co	10	20	0.24
$La_{0.7}Sr_{0.3}CrO_3$[7]	Ni	20	4	0.31

References

1 Liu, S. B., Chuang, K. T. & Luo, J. L. Double-layered perovskite anode with in situ exsolution of a Co–Fe alloy to cogenerate ethylene and electricity in a proton-conducting ethane fuel cell. *ACS Catalysis* **6**, 760-768 (2015).

2 Fu, L. et al. Exsolution of Cu nanoparticles in $(LaSr)_{0.9}Fe_{0.9}Cu_{0.1}O_4$ Ruddlesden-Popper oxide as symmetrical electrode for solid oxide cells. *Applied Surface Science* **511**, 145525 (2020).

3 Li, H. D. et al. Exsolved alloy nanoparticles decorated Ruddlesden–Popper perovskite as sulfur-tolerant anodes for solid oxide fuel cells. *Energy & Fuels* **34**, 11449-11457 (2020).

4 Ni, C. S. et al. A B-site doped perovskite ferrate as an efficient anode of a solid oxide fuel cell with in situ metal exsolution. *Journal of Materials Chemistry A* **7**, 26944-26953 (2019).

5 Kang, B. S., Matsuda, J. & Ishihara, T. Cu–Fe–Ni nano alloy particles obtained by exsolution from $Cu(Ni)Fe_2O_4$ as active anode for SOFCs. *Journal of Materials Chemistry A* **7**, 26105-26115 (2019).

6 Zhou, J. et al. In situ growth of nanoparticles in layered perovskite $La_{0.8}Sr_{1.2}Fe_{0.9}Co_{0.1}O_{4-\delta}$ as an active and stable electrode for symmetrical solid oxide fuel cells. *Chemistry of Materials* **28**, 2981-2993 (2016).

7 Sun, Y. F. et al. A-site deficient perovskite: the parent for in situ exsolution of highly active, regenerable nano-particles as SOFC anodes. *Journal of Materials Chemistry A* **3**, 11048-11056 (2015).